

Circularly Polarized Wearable Antenna With Low Profile and Low Specific Absorption Rate Using Highly Conductive Graphene Film

Hao-Ran Zu ^{1b}, Bian Wu ^{1b}, *Member, IEEE*, Ya-Hui Zhang ^{1b}, Yu-Tong Zhao, Rong-Guo Song, and Da-Ping He ^{1b}

Abstract—A low-profile circularly polarized wearable antenna with flexible performance and reduced specific absorption rate (SAR) based on graphene is presented. The antenna adopts highly conductive graphene film and polydimethylsiloxane substrate, which have good flexibility, mechanical stability, and light weight. The wearable antenna operating at 5.8 GHz with a profile of 0.05λ is designed and fabricated, which retains a reflection coefficient of less than -10 dB when loaded on the human body. The measured results indicate the axial-ratio (AR) bandwidth for $AR < 3$ dB covers 5.75–5.83 GHz with the realized gain varying from 5.0–6.1 dBic. The SAR peak is 1.02 W/kg when the human tissue is 1g and 0.947 W/kg when the human tissue is 10g, which meets the international SAR standards.

Index Terms—Circularly polarized, highly conductive graphene film (CGF), low profile, specific absorption rate (SAR), wearable antenna.

I. INTRODUCTION

NOVEL wireless communication system based on body area network is emerging in our daily life to meet the increased requirements of intelligent telemedicine and health monitoring, where wearable devices play a significant role [1]. In wireless on body area networks, devices need to satisfy some special performances, such as wearability, flexibility, low profile, and low specific absorption rate (SAR). Therefore, substantial research on wearable devices has been carried on, especially the antenna design [2]–[4].

The wearable antenna based on flexible substrates has drawn lots of attention since they are bendable when their soft substrates are clad by the thin metallic film. However, with the improved performance requirements of wearable antennas, such

as light weight, flexural endurance and corrosion resistance, traditional metallic materials are not good candidates. Recently, novel conductive materials have attracted increasing attention. There are several types of novel conductive materials, such as metal nanoparticle, conductive polymer, and carbon nanotube. Nevertheless, the metal nanoparticle is too expensive and easy to be oxidized [5], the conductive polymer normally has low conductivity which is not suitable for antenna design [6], and the carbon nanotube also has relatively high sheet resistance resulting from junction resistance [7]. Recently, the highly conductive graphene film (CGF) has been proposed as a promising alternative conducting material for antenna design [8] and sensing applications [9]. This kind of carbon-based film possesses many advantages including high conductivity, excellent flexural endurance, chemical stability and environmental friendliness, which is discussed in our previous works [10]–[12]. The superiorities of highly CGFs show great potential in overcoming the challenges of wearable antenna design.

The existing wearable antennas can be generally divided into several types: monopole form [13]–[15], microstrip patch form [16], [17], monopole combined with artificial magnetic conductor (AMC) [18]–[20] and others [21]–[23]. In the case of single-layer antennas, such as monopole and dipole, it usually has no back-metal to achieve isolation between the antenna and the human body, which leads to high SAR. The AMC-based wearable antenna can solve the excessive SAR problem. However, this multilayer structure increases the overall thickness. The previous AMC-based wearable antennas proposed in [18]–[20], [24] have an exceeding thickness of 4 mm and operate in linear polarization, which cannot guarantee the antenna performance in motion. In summary, it remains a big challenge to realize a wearable antenna with a low profile, low SAR, and circular polarization.

In this letter, we propose a novel circularly polarized flexible antenna with both low profile and low SAR by using highly CGF. To the best of our knowledge, the CGF is applied to the wearable antenna for the first time, and it is proved to have good flexibility and mechanical stability as well as high conductivity. The proposed graphene-based antenna achieves circular polarization with low SAR and low profile of 2.57 mm in the Industrial, Scientific, and Medical (ISM) radio band. A practical antenna is fabricated, and the antenna performance is measured at different body positions of the human body. The measurement results validate the simulations.

II. CHARACTERIZATION OF THE CGF

The carbon-based film exhibits more favorable properties than most metal materials in flexibility, mechanical reliability, light

Manuscript received September 21, 2020; revised October 12, 2020; accepted October 17, 2020. Date of publication October 22, 2020; date of current version December 22, 2020. This work was supported in part by the National Natural Science Foundation of China under Grant 61771360, Grant U19A2055, Grant 61701349, and Grant 62071357; in part by the Key Industry Chain Project of Shaanxi Province under Grant 2018ZDCXL-GY-08-03-01; in part by the Key Laboratory Foundation under Grant 6142216180104; and in part by the Fundamental Research Funds for the Central Universities and the Innovation Fund of Xidian University. (*Corresponding author: Bian Wu; Yu-Tong Zhao.*)

Hao-Ran Zu, Bian Wu, Ya-Hui Zhang, and Yu-Tong Zhao are with the Key Laboratory of Antennas and Microwave Technology, Xidian University, Xi'an 710071, China (e-mail: zuhr@foxmail.com; bwu@mail.xidian.edu.cn; 757613302@qq.com; 981554667@qq.com).

Rong-Guo Song and Da-Ping He are with the Engineering Research Center of RF-Microwave Technology and Application, Wuhan University of Technology, Wuhan 430070, China (e-mail: rongguo_song@whut.edu.cn; hedaping@whut.edu.cn).

Digital Object Identifier 10.1109/LAWP.2020.3033013

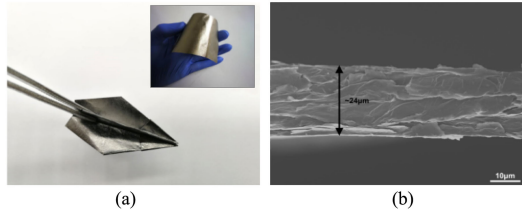


Fig. 1. (a) Photographs of the CGF. (b) Cross-section SEM image of the CGF.

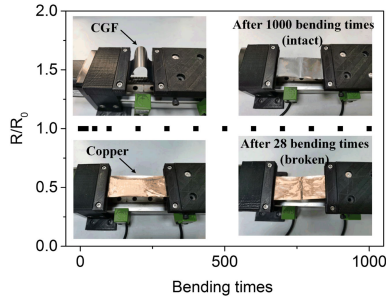


Fig. 2. Comparative experiment of mechanical reliability between the CGF and copper.

weight, and excellent environmental toughness [10]–[12]. We have presented and realized a kind of CGF with high conductivity and excellent flexural endurance in [8] and [10], which shows superiorities in the wearable application. Fig. 1 illustrates the photographs and the cross-section scanning electron microscopy (SEM) image of the CGF sample, which has good flexibility and can be bent and folded into an airplane. The CGF is fabricated by three steps: vacuumed heating; firing under argon atmosphere; and rolling process, which is described in detail in our previous work [8] and [10]. After the rolling process, the CGF shows a glossy surface, which means the regularity of graphene sheets and the density of the CGF is improved [8], [10]. The cross-section SEM image shows the thickness of CGF is $\sim 24 \mu\text{m}$, the corresponding electrical conductivity is $1.13 \times 10^6 \text{ S/m}$, which is very close to the electrical conductivity of metal and has the potential for antenna design. Moreover, the density of the CGF is 1.8 g/cm^3 , which is smaller than a quarter of the copper density of 8.8 g/cm^3 , a light weight is easy to be achieved.

The comparative experiment of mechanical reliability between the CGF and copper is exhibited in Fig. 2. The CGF can restore to its original state without any damage after folding and kneading. Furthermore, the CGF can maintain unchanged resistivity after 1000 bending cycles at a frequency of 0.5 Hz, while commercial copper foil broke after only 28 cycles due to metal fatigue, which proves that the CGF has good flexibility and better mechanical stability than the traditional metallic materials. Therefore, the proposed carbon-based CGF behaves excellently under flexural endurance, has light weight and high conductivity, which is suitable for flexible and conformal antenna applications in the wearable communication system.

III. CONFIGURATION AND PRINCIPLE

Making use of the advantages of the presented CGF above, we aim to realize a low-profile and circular polarization wearable antenna based on the CGF. The working frequency is chosen as 5.8 GHz (5.75–5.83 GHz) within the ISM band. The structure of the proposed wearable antenna is shown in Fig. 3, which

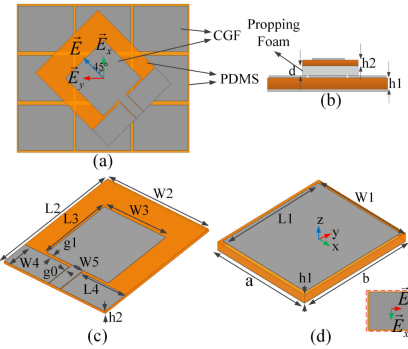


Fig. 3. Structure of the proposed wearable antenna. (a) Top view. (b) Side view. (c) Structure of the monopole patch. (d) Structure of the unit cell of the AMC array.

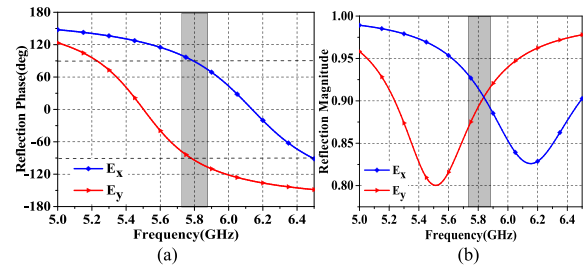


Fig. 4. (a) Reflection phase and (b) reflection magnitude of the proposed AMC.

consists of a monopole patch, a 3×3 AMC array and a propping foam. The propping foam adopts ROHACELL 71HF with a dielectric constant of 1.075 and the loss tangent of 0.0002, and the monopole patch and AMC array employ CGF as the conductive material. The monopole patch is placed at an angle of 45° above the AMC array, and the thickness of propping foam is $d = 1 \text{ mm}$. Both the monopole patch and the AMC array use the flexible polydimethylsiloxane (PDMS) as the substrates with a dielectric constant of 2.7 and the loss tangent of 0.013, while the thickness of the PDMS substrate for them is $h1 = 1 \text{ mm}$ and $h2 = 0.5 \text{ mm}$, respectively. The monopole patch is fed by a coplanar waveguide with 50Ω characteristic impedance.

The AMC array placed on the back of the monopole patch is designed to modulate the reflected wave and protect the human body against the harm of electromagnetic radiation. When the reflection phases in x -direction and y -direction of the AMC array equal 90° and -90° , a right-hand circular polarization (RHCP) can be achieved [25]. Fig. 4 shows the reflection phase and reflection magnitude of the AMC unit cell. Around the working frequency of 5.8 GHz, the reflection phases in x -direction and y -direction are 90° and -90° , respectively, while the reflection magnitude has little difference, which means the RHCP can be obtained.

Therefore, we can utilize the designed anisotropic AMC array incorporating with monopole radiation patch to achieve RHCP of the whole wearable antenna. The geometrical parameters of the proposed antenna are given in Table I.

IV. ANTENNA PERFORMANCE ON HUMAN BODY

Since the wearable antenna needs to conform to the tissue surface of the human body, the performance of the proposed antenna under different bending radii needs to be considered. We set the bending radii of $R = 100$ and 30 mm in two orthometric

TABLE I
GEOMETRICAL PARAMETERS OF THE PROPOSED WEARABLE ANTENNA

Parameter	h_1	h_2	d	L_2	L_3	W_2	a	b
Value(mm)	1	0.5	1	27	13.9	23	12.9	15
Parameter	W_3	W_4	W_5	g_0	g_1	L_4	W_1	L_1
Value(mm)	14	5.4	2.5	0.15	0.6	10.1	11.8	14.3

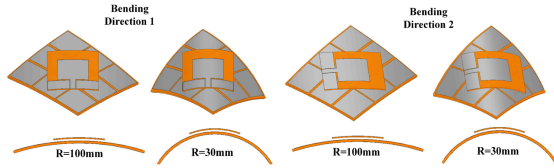


Fig. 5. Proposed wearable antenna under different bending radii in two orthometric bending directions.

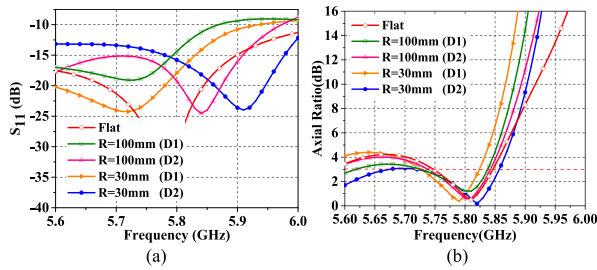


Fig. 6. (a) Reflection coefficient and (b) axial ratio of the wearable antenna under flat and bending states.

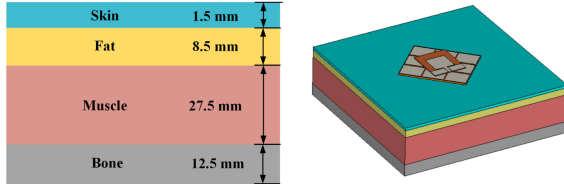


Fig. 7. Wearable antenna loaded on the human body model.

bending directions as shown in Fig. 5 to model the cases on the chest and wrist of an adult body. As shown in Fig. 6, the reflection coefficients corresponding to different bending radii in two orthometric bending directions ($D1$ and $D2$) remain below -10 dB within the ISM frequency band of 5.8 GHz. The antenna can guarantee circular polarization between 5.75 and 5.83 GHz for all bending conditions, which includes the antenna being flat and bent to different radii and in different directions. These results indicate that both the impedance matching and the circular polarization are guaranteed under different bending radii.

In order to evaluate the impact of the human body, the radiation performance of the proposed antenna in direct contact with the body and free space is simulated. As shown in Fig. 7, a multilayer human tissue model was employed to mimic the human arm, with a dimension of 120 mm \times 120 mm \times 50 mm. This model consists of four layers representing skin, fat, muscle, and bone tissues [26], and the typical permittivity, conductivity and mass density values have been reported in [27].

Fig. 8 depicts the simulated reflection coefficients and the axial ratio of the antenna in free space and in direct contact with the human body, which shows good agreement. The simulated

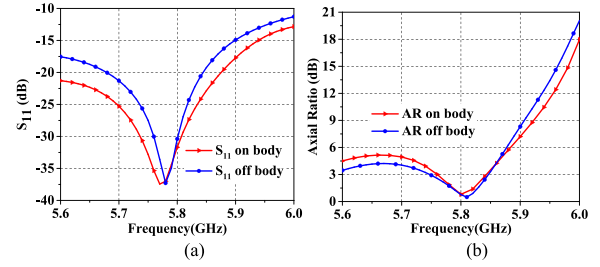


Fig. 8. (a) Reflection coefficient and (b) axial ratio of the wearable antenna on and off the human body.

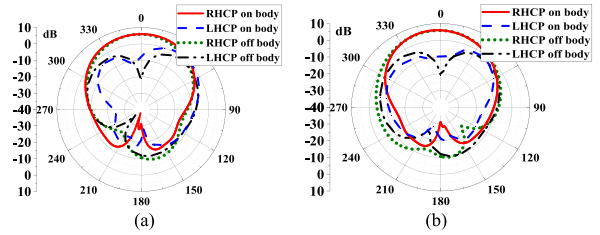


Fig. 9. The radiation patterns of the wearable antenna on/off human body. (a) xoz plane. (b) $yo z$ plane.

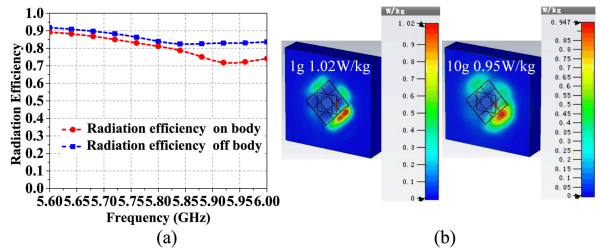


Fig. 10. (a) Radiation efficiency of the wearable antenna on/off human body. (b) Simulated SAR value of the wearable antenna with human body.

radiation patterns and radiation efficiency are displayed in Figs. 9 and 10(a), respectively. When the antenna is placed on the human body, the RHCP radiation patterns in the xoz plane and $yo z$ plane remain almost the same with that in free space. The RHCP gain is more than 15 dB higher than the left-hand circular polarization (LHCP) gain in the 0° direction in both planes. Besides, the gain of the antenna at 0° increases a little, and decreases at 180° when it is placed on the human body, which is mainly caused by the body reflection of the electromagnetic energy. The radiation efficiencies of the on-body and off-body wearable antenna are displayed in Fig. 10, which are over 70% under both conditions.

For wearable applications, the radiation safety of the wearable antenna must be considered. The SAR is generally used to characterize the rate of the electromagnetic energy absorbed by the human tissues. The FCC and ICNIRP stipulate that the SAR value cannot exceed 1.6 and 2 W/kg for 1 and 10 g human tissue, respectively. As depicted in Fig. 10 (b), the SAR is calculated with the input power of 500 mW, and a maximum 1 g SAR value of 1.02 W/kg and a maximum 10 g SAR value of 0.95 W/kg are achieved. Therefore, to satisfy the FCC and ICNIRP standards, the maximum input power has to be kept lower than approximately 784 mW. Complying with the regulations of FCC and ICNIRP, the proposed antenna is safe for wearable applications.

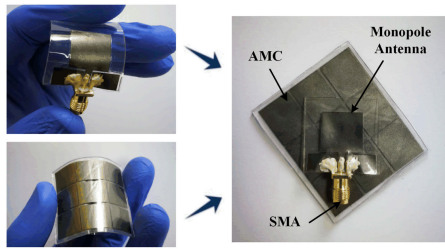


Fig. 11. Photographs of the CGF wearable antenna.

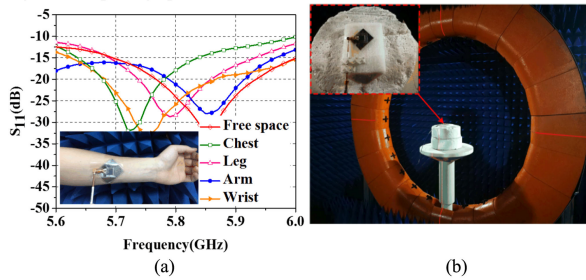
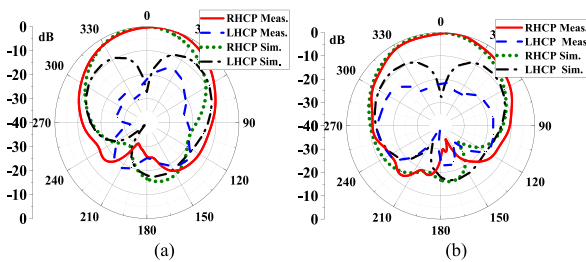


Fig. 12. (a) Measured reflection coefficients in different positions of the body. (b) Photograph of the measurement environment.

Fig. 13. Simulated and measured radiation patterns of the wearable antenna at 5.8 GHz. (a) xoz plane. (b) $yo z$ plane.

V. FABRICATION AND MEASUREMENTS OF ANTENNA

As shown in Fig. 11, the monopole patch of the wearable antenna electrically connects to the subminiature version A (SMA) connector through the conductive adhesive. The conductive adhesive adopts silver colloidal suspension 05001-AB from the structure probe incorporated company, and the typical sheet resistivity is $12 \text{ m}\Omega/\text{square}$. The monopole patch layer is placed above the AMC array layer by a piece of 1 mm thick foam as an upholder. The fabricated antenna has good flexibility and the total thickness is only 2.57 mm.

To verify the practical performance of the wearable antenna, the fabricated antenna was measured by a vector network analyzer while attached to different positions of the human body including the chest, arm, twist, and leg, and the measured reflection coefficients are compared in Fig. 12(a). Although the resonance depth and center frequency show some little changes in different body positions, the impedance bandwidth for $S_{11} < -10 \text{ dB}$ covers 5.6–6.0 GHz consistently, which means the antenna remains good impedance matching in different positions of the human body.

The radiation performance of CGF wearable antenna was measured in an anechoic chamber as shown in Fig. 12(b). Fig. 13 presents the simulated and measured radiation patterns in the xoz plane and $yo z$ plane. The RHCP gain is more than 20 dB

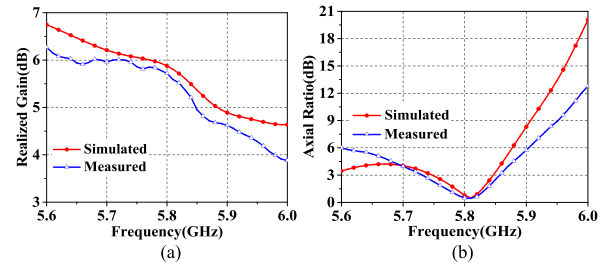


Fig. 14. Simulated and measured realized gain and axial ratio of the wearable antenna. (a) Realized gain. (b) Axial ratio.

TABLE II
COMPARISON OF PROPOSED ANTENNA WITH OTHER WEARABLE ANTENNAS

Ref.	Profile (mm) (5.8 GHz)	Polarization Mode	SAR (1g/10g W/Kg)	Gain (dBi)	Material (conductive/dielectric)
[20]	5.52	Linear	0.31/0.08	7.7	Copper/Ro3003 & 3850
[24]	6.1	Linear	0.75/0.28	7.7	Copper/Polyimide
[26]	3.6	Linear	0.56/1.18	6.1	Copper Taffeta/Pellon
[28]	12	LHCP	NA	3.9	Textile & Copper/FR4
[29]	2	Linear	0.93/0.40	5.9	Conductive Fabric/Wool Felt,
Our work	2.57	RHCP	1.02/0.95	6.0	CGF/PDMS

higher than LHCP gain in the 0° direction in both planes, which indicates the fabricated antenna has good polarization isolation. As demonstrated in Fig. 14, the simulated and measured results of realized gain and the axial ratio of the proposed antenna show good consistency. Within 5.75–5.83 GHz, the measured realized gain ranges from 5.0–6.1 dBic, and the axial ratio is less than 3 dB. The measured results verify the proposed antenna with a low profile and low SAR possesses good RHCP performance, high polarization isolation, and stable gain, which is suitable for on-body wireless communication.

Table II gives the comparison between the proposed wearable antenna and the recently published wearable antennas. It can be concluded that the proposed antenna provides one of the lowest profile and circular polarization with an acceptable SAR and a mid-range gain. This letter offers a method to achieve low profile, circular polarization, and safe SAR in wearable antenna design. Moreover, using CGF as conductive film and PDMS as dielectric substrate guarantees flexibility, mechanical stability, and light weight of the wearable antenna.

VI. CONCLUSION

A novel circularly polarized wearable antenna with low profile and low SAR using highly CGF is designed, fabricated and measured, which also possesses many mechanical advantages, such as good flexibility and excellent flexural endurance. The CGF antenna has only 2.57 mm profile and achieves RHCP with high polarization isolation. Within 5.75–5.83 GHz, the axial ratio is less than 3 dB, the reflection coefficient is less than -15 dB , and the realized gain ranges from 5.0–6.1 dBic, which works in the ISM radio band. The CGF wearable antenna shows superiorities and good potential in the on-body communication system.

REFERENCES

- [1] S. Han and S. K. Park, "Performance analysis of wireless body area network in indoor off-body communication," *IEEE Trans. Consum. Electron.*, vol. 57, no. 2, pp. 335–338, May 2011.
- [2] M. Hirvonen, C. Böhme, D. Severac, and M. Maman, "On-body propagation performance with textile antennas at 867 MHz," *IEEE Trans. Antennas Propag.*, vol. 61, no. 4, pp. 2195–2199, Apr. 2013.
- [3] M. Virili, H. Rogier, F. Alimenti, P. Mezzanotte, and L. Roselli, "Wearable textile antenna magnetically coupled to flexible active electronic circuits," *IEEE Antennas Wireless Propag. Lett.*, vol. 13, pp. 209–212, 2014.
- [4] S. Agneessens, S. Lemey, T. Vervust, and H. Rogier, "Wearable small and robust: The circular quarter-mode textile antenna," *IEEE Antennas Wireless Propag. Lett.*, vol. 14, pp. 1482–1485, 2015.
- [5] R. Doering and Y. Nishi, *Handbook of Semiconductor Manufacturing Technology*, Boca Raton, FL, USA: CRC Press, 2007.
- [6] A. Kamyshny and S. Magdassi, "Conductive nanomaterials for printed electronics," *Small*, vol. 10, no. 17, pp. 3515–3535, 2014.
- [7] S. Hellstrom, H. Lee, and Z. Bao, "Polymer-Assisted direct deposition of uniform carbon nanotube bundle networks for high performance transparent electrodes," *ACS Nano*, vol. 3, no. 6, pp. 1423–1430, 2009.
- [8] C. Fan, B. Wu, R. Song, Y. Zhao, Y. Zhang, and D. He, "Electromagnetic shielding and multi-beam radiation with high conductivity multilayer graphene film," *Carbon*, vol. 155, pp. 506–513, 2019.
- [9] T. Leng *et al.*, "Graphene nanoflakes printed flexible meandered-line dipole antenna on paper substrate for low-cost RFID and sensing applications," *IEEE Antennas Wireless Propag. Lett.*, vol. 15, pp. 1565–1568, 2016.
- [10] R. Song *et al.*, "Flexible graphite films with high conductivity for radio-frequency antennas," *Carbon*, vol. 130, pp. 164–169, Apr. 2018.
- [11] R. Song *et al.*, "Sandwiched graphene clad laminate: A binder-free flexible printed circuit board for 5G antenna application," *Adv. Eng. Mater.*, vol. 22, 2020, Art. no. 2000451.
- [12] W. Zhou *et al.*, "Flexible radiofrequency filters based on highly conductive graphene assembly films," *Appl. Phys. Lett.*, vol. 114, 2019, Art. no. 113503.
- [13] Z. Hamouda *et al.*, "Dual-band elliptical planar conductive polymer antenna printed on a flexible substrate," *IEEE Trans. Antennas Propag.*, vol. 63, no. 12, pp. 5864–5867, Dec. 2015.
- [14] B. Hu, G. Gao, L. He, X. Cong, and J. Zhao, "Bending and on-arm effects on a wearable antenna for 2.45 GHz body area network," *IEEE Antennas Wireless Propag. Lett.*, vol. 15, pp. 378–381, 2016.
- [15] Z. Hamouda, J. Wojkiewicz, A. A. Pud, L. Koné, S. Bergheul, and T. Lasri, "Magnetodielectric nanocomposite polymer-based dual-band flexible antenna for wearable applications," *IEEE Trans. Antennas Propag.*, vol. 66, no. 7, pp. 3271–3277, Jul. 2018.
- [16] C. Lin, C. Chang, Y. T. Cheng, and C. F. Jou, "Development of a flexible SU-8/PDMS-based antenna," *IEEE Antennas Wireless Propag. Lett.*, vol. 10, pp. 1108–1111, 2011.
- [17] C. Mendes and C. Peixeiro, "A dual-mode single-band wearable microstrip antenna for body area networks," *IEEE Antennas Wireless Propag. Lett.*, vol. 16, pp. 3055–3058, 2017.
- [18] X. Liu, Y. Di, H. Liu, Z. Wu, and M. M. Tentzeris, "A planar windmill-like broadband antenna equipped with artificial magnetic conductor for off-body communications," *IEEE Antennas Wireless Propag. Lett.*, vol. 15, pp. 64–67, 2016.
- [19] K. Agarwal, Y. Guo, and B. Salam, "Wearable AMC backed near-endfire antenna for on-body communications on latex substrate," *IEEE Trans. Compon., Packag., Manuf. Technol.*, vol. 6, no. 3, pp. 346–358, Mar. 2016.
- [20] M. E. Atrash, M. A. Abdalla, and H. M. Elhennawy, "A wearable dual-band low profile high gain low SAR antenna AMC-backed for WBAN applications," *IEEE Trans. Antennas Propag.*, vol. 67, no. 10, pp. 6378–6388, Oct. 2019.
- [21] R. B. V. B. Simorangkir, A. Kiourti, and K. P. Esselle, "UWB wearable antenna with a full ground plane based on PDMS-embedded conductive fabric," *IEEE Antennas Wireless Propag. Lett.*, vol. 17, no. 3, pp. 493–496, Mar. 2018.
- [22] A. S. M. Alqadami, N. Nguyen-Trong, B. Mohammed, A. E. Stancombe, M. T. Heitzmann, and A. Abbosh, "Compact unidirectional conformal antenna based on flexible high-permittivity custom-made substrate for wearable wideband electromagnetic head imaging system," *IEEE Trans. Antennas Propag.*, vol. 68, no. 1, pp. 183–194, Jan. 2020.
- [23] A. Arif, M. Zubair, M. Ali, M. U. Khan, and M. Q. Mehmood, "A compact, low-profile fractal antenna for wearable on-body WBAN applications," *IEEE Antennas Wireless Propag. Lett.*, vol. 18, no. 5, pp. 981–985, May 2019.
- [24] M. Wang *et al.*, "Investigation of SAR reduction using flexible antenna with metamaterial structure in wireless body area network," *IEEE Trans. Antennas Propag.*, vol. 66, no. 6, pp. 3076–3086, Jun. 2018.
- [25] F. Yang and Y. Rahmat-Samii, "A low profile single dipole antenna radiating circularly polarized waves," *IEEE Trans. Antennas Propag.*, vol. 53, no. 9, pp. 3083–3086, Sep. 2005.
- [26] A. Alemarveen and S. Noghianian, "On-body low-profile textile antenna with artificial magnetic conductor," *IEEE Trans. Antennas Propag.*, vol. 67, no. 6, pp. 3649–3656, Jun. 2019.
- [27] M. A. Stuchly and S. S. Stuchly, "Dielectric properties of biological substances-tabulated," *J. Microw. Power*, vol. 15, no. 1, pp. 19–26, Jan. 1980.
- [28] X. Hu, S. Yan, and G. A. E. Vandenbosch, "Compact circularly polarized wearable button antenna with broadside pattern for U-NII worldwide band applications," *IEEE Trans. Antennas Propag.*, vol. 67, no. 2, pp. 1341–1345, Feb. 2019.
- [29] G. Gao, C. Yang, B. Hu, R. Zhang, and S. Wang, "A wide-bandwidth wearable all-textile PIFA with dual resonance modes for 5 GHz WLAN applications," *IEEE Trans. Antennas Propag.*, vol. 67, no. 6, pp. 4206–4211, Jun. 2019.